

The matrix permanent and determinant from a spin system

Abhijeet Alase

Quantum Science Group, The University of Sydney, NSW 2006, Australia

Owen Doty and David L. Feder

*Institute for Quantum Science and Technology and Department of Physics and Astronomy,
University of Calgary, Calgary, Alberta T2N 1N4, Canada*

In contrast to the determinant, no algorithm is known for the exact determination of the permanent of a square matrix that runs in time polynomial in its dimension. Consequently, non-interacting fermions are classically efficiently simulatable while non-interacting bosons are not, underpinning quantum supremacy arguments for sampling the output distribution of photon interferometer arrays. This work introduces a graph-theoretic framework that bridges both the determinant and permanent. The only non-zero eigenvalues of a sparse non-Hermitian operator \tilde{M} for n spin-1/2 particles are the n th roots of the permanent or determinant of an $n \times n$ matrix M , interpreting basis states as bosonic or fermionic occupation states, respectively. This operator can be used to design a simple and straightforward method for the classical determination of the permanent that matches the efficiency of the best-known algorithm. Gauss-Jordan elimination for the determinant of M is then equivalent to the successive removal of the generalized zero eigenspace of the fermionic \tilde{M} , equivalent to the deletion of some nodes and reweighting of the remaining edges in the graph such that only n nodes survive after the last step. In the bosonic case, the successive removal of generalized zero eigenspaces for \tilde{M} is also equivalent to node deletion, but new edges are added during this process, which gives rise to the higher complexity of computing the permanent. Our analysis may point the way to new strategies for classical and quantum evaluation of the permanent.

I. INTRODUCTION

The permanent of a square matrix M of dimension n is the symmetric analogue of the usual determinant, but where the signatures of the permutations (the signs appearing in the expansion of the function) are ignored. This quantity appears in a wide variety of applications in pure mathematics and in physics, among other disciplines. For example, the permanent enumerates the number of perfect matchings of a bipartite graph, which has applications in combinatorics [1], chemistry [2], and physics [3]. The permanent arises in the identification of multiple targets [4], with applications to defense. In the context of quantum computation and information, the permanent is central to calculating matrix elements in linear optics for many-photon systems [5–7], and for determining the entanglement of various permutation-invariant quantum states [8].

Despite the fact that both the permanent and the determinant yield the same exponential number of terms, $n! \sim \sqrt{2\pi n}(n/e)^n$ for large n , the determinant is efficiently computable classically, i.e. scales as a polynomial in n . The well-known Gaussian elimination approach scales as $O(n^3)$, and the fastest current algorithm scales as $O(n^{2.373})$ [9]. In contrast, determining the permanent of a general matrix is #P-hard, and that of a $(0, 1)$ matrix is #P-complete [10–12]. The discovery of a classically efficient algorithm for the permanent would have profound consequences for the theory of computation, including $P = PP$ [13], an even stronger statement than the famous $P = NP$ conjecture. The runtime of the fastest known algorithm, namely Ryser’s algorithm, scales as $O(n2^n)$ [14, 15]. That said, the permanent P_n of ma-

trices with non-negative entries or with vanishing mean can be *approximated* in polynomial time $\text{poly}(n, 1/\epsilon)$ using randomized algorithms [16, 17], up to additive error ϵP_n , for arbitrary $\epsilon > 0$; likewise for positive semidefinite matrices [18–20].

The #P-hardness of computing the permanent was recast in the framework of linear optics [6], which motivated the realization that quantum devices will always outperform classical algorithms in sampling the output distribution of photons emerging from an optical interferometer apparatus, the so-called Boson Sampling problem [7]. Numerous Boson Sampling experiments have been conducted since then; Refs. 21–23 provide some recent examples. In contrast, the ease of calculating the determinant implies that non-interacting fermions are efficiently simulatable on a classical computer [24–28].

It was recently shown that the permanent of the matrix M can be computed as the determinant of a family of matrices \tilde{M} of minimum dimension $2^n - 1$ [29–31]. These matrices define the adjacency of a directed n -dimensional hypercube graph, whose edge weights correspond to elements of the matrix of interest, and with the first and last vertices sharing the same label to form a cycle. It was subsequently noted that these graphs encode an algebraic branching program [32]: the product of edge weights on each of the $n!$ possible branches corresponds to a term in the expansion of the permanent.

The present work builds on the above construction by identifying a key feature: the structure of the matrix M coincides with the dynamics of n spin-1/2 particles governed by a non-Hermitian operator. If the permanent of M is non-zero, then the only non-zero eigenvalues of \tilde{M} are the n th roots of the permanent; alternatively, \tilde{M}^n di-

agonalizes into n blocks labeled by the total spin, each of which has the permanent as the only non-zero eigenvalue. Thus, the n -fold product of \tilde{M} on a fiducial state such as $|0^{\otimes n}\rangle$ immediately yields $P_n|0^{\otimes n}\rangle$. The n -sparsity of \tilde{M} ensures that this can be effected on a classical computer with $n2^n$ arithmetic operations, matching the performance of Ryser's algorithm.

Interpreting the basis states as bosonic occupation states yields the standard expression for the permanent in terms of products of (hard-core) bosonic operators. Interpreting these instead as fermionic occupation states immediately yields the determinant, with signed edge weights in the graph. If M is a full-rank matrix, then Gaussian elimination for the calculation of the determinant corresponds to successively projecting out the generalized zero eigenvectors of \tilde{M} , so that after n iterations the initial rank-deficient matrix of dimension $2^n - 1$ is reduced to an n -dimensional full-rank matrix. From the perspective of the algebraic branching program, each iteration deletes vertices and the edges incident to them, and reweights the remaining edges, until only one path remains in the cycle. This approach uncovers another close connection between fermions and the determinant on the one hand, and between bosons and the permanent on the other.

This paper is organized as follows. The permanent and determinant are reviewed in Sec. II, and an example is provided for the representation of the permanent as an algebraic branching program. Sec. III introduces the spin model that maps the problem of computing the permanent of an $n \times n$ matrix M to the problem of computing the eigenvalues of a $2^n \times 2^n$ matrix \tilde{M} , and provides a classical algorithm for computing the permanent that matches the best current methods. The spin model is expressed in terms of non-interacting fermions and hard-core bosons in Sec. IV. In Sec. V, we discuss the connection between Gaussian elimination, generalized zero eigenspaces of \tilde{M} and its visualization on the associated graph. The prospects for the development of a quantum algorithm for computing the permanent based on our approach are discussed in Sec. VI.

II. REVIEW

A. Permanent and determinant

Consider the $n \times n$ matrix M , defined as

$$M = \begin{pmatrix} w_{0,0} & w_{0,1} & \cdots & w_{0,n-1} \\ w_{1,0} & w_{1,1} & \cdots & w_{1,n-1} \\ \vdots & \vdots & \ddots & \vdots \\ w_{n-1,0} & w_{n-1,1} & \cdots & w_{n-1,n-1} \end{pmatrix}. \quad (1)$$

The determinant and permanent of M are respectively defined as

$$D_n = |M| = \det(M) \equiv \sum_{\sigma \in S_n} \left(\text{sgn}(\sigma) \prod_{i=0}^{n-1} w_{i,\sigma_i} \right);$$

$$P_n = |M|_P = \text{perm}(M) \equiv \sum_{\sigma \in S_n} \left(\prod_{i=0}^{n-1} w_{i,\sigma_i} \right),$$

where S_n is the symmetric group on the list $\{0, 1, 2, \dots, n-1\}$, σ is a function that reorders this list (effects a permutation of the elements), σ_i is the i th entry of the list after permutation, and $\text{sgn}(\sigma) = (-1)^{N(\sigma)}$ is the signature of the permutation, where $N(\sigma)$ is the number of inversions needed. While the expansion of the determinant and permanent includes the same $n!$ terms, the signs appearing in the determinant allow for its efficient evaluation.

While exceedingly simple, the $n = 3$ case is illustrative and will be revisited throughout this work. The determinant is explicitly written

$$\begin{aligned} |M| &= w_{0,0}(w_{1,1}w_{2,2} - w_{1,2}w_{2,1}) \\ &- w_{0,1}(w_{1,0}w_{2,2} - w_{1,2}w_{2,0}) \\ &+ w_{0,2}(w_{1,0}w_{2,1} - w_{1,1}w_{2,0}). \end{aligned} \quad (2)$$

The Gaussian elimination algorithm uses pivoting to reduce the matrix to row echelon form (i.e. an upper triangular matrix), so that the determinant is the product of the diagonal elements. For reasons that will become clear in Sec. IV, consider instead a reduction to a lower triangular matrix. The first reduction yields

$$|M| = \begin{vmatrix} w'_{0,0} & w'_{0,1} & 0 \\ w'_{1,0} & w'_{1,1} & 0 \\ w_{2,0} & w_{2,1} & w_{2,2} \end{vmatrix}, \quad (3)$$

where

$$w'_{0,0} = w_{0,0} - \frac{w_{0,2}w_{1,0}}{w_{1,2}}; \quad w'_{0,1} = w_{0,1} - \frac{w_{0,2}w_{1,1}}{w_{1,2}}; \quad (4)$$

$$w'_{1,0} = w_{1,0} - \frac{w_{1,2}w_{2,0}}{w_{2,2}}; \quad w'_{1,1} = w_{1,1} - \frac{w_{1,2}w_{2,1}}{w_{2,2}}. \quad (5)$$

The second and last reduction yields

$$|M| = \begin{vmatrix} w''_{0,0} & 0 & 0 \\ w'_{1,0} & w'_{1,1} & 0 \\ w_{2,0} & w_{2,1} & w_{2,2} \end{vmatrix}, \quad (6)$$

where

$$w''_{0,0} = w'_{0,0} - \frac{w'_{0,1}w'_{1,0}}{w'_{1,1}}. \quad (7)$$

The determinant is then

$$\begin{aligned} |M| &= w''_{0,0}w'_{1,1}w_{2,2} = (w'_{0,0}w'_{1,1} - w'_{0,1}w'_{1,0})w_{2,2} \\ &= \left(w_{0,0} - \frac{w_{0,2}w_{1,0}}{w_{1,2}} \right) \left(w_{1,1} - \frac{w_{1,2}w_{2,1}}{w_{2,2}} \right) \\ &- \left(w_{0,1} - \frac{w_{0,2}w_{1,1}}{w_{1,2}} \right) \left(w_{1,0} - \frac{w_{1,2}w_{2,0}}{w_{2,2}} \right) w_{2,2}. \end{aligned} \quad (8)$$

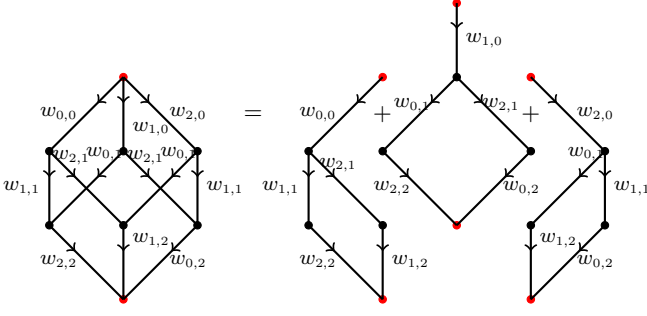


FIG. 1. (Color online) Illustration of the algebraic branching program for the evaluation of the permanent $|M|_P$ for $n = 3$.

While there are eight terms in the expansion, the signs the two cross terms $\left(-\frac{w_{0,2}w_{1,0}}{w_{1,2}}\right)(w_{1,1})w_{2,2}$ and $-\left(-\frac{w_{0,2}w_{1,1}}{w_{1,2}}\right)(w_{1,0})w_{2,2}$ cancel, leaving 6 unique terms in the expansion.

The sign structure of the determinant guarantees that these cancellations occur for all values of n , which ensures that Gaussian elimination is classically efficient. For the evaluation of the permanent, one cannot follow the same procedure as above by simply eliminating all signs, because the cross terms arising from expanding the final product [for example in Eq. (8)] will now add instead of cancelling. Our analysis in Sec. VB provides insight into why this is the case.

B. Permanent as an algebraic branching program

Building on the work of Grenet and others [29–31], Hüttenhain and Ikenmeyer [32] noted that the matrix permanent for $n = 3$ can be expressed as a binary algebraic branching program. The $n!$ terms correspond to branches, or routes, traversing between antipodes of the n -dimensional hypercube, such that the product of edge weights for each branch corresponds to a term in the expansion of the permanent. Fig. 1 illustrates the idea for the $n = 3$ case, where the three main branches from the top to bottom vertices (labeled in red) are explicitly shown. The edge weights are chosen so that their products for each branch correspond to a term in the permanent; c.f. Eq. (2) with signs removed. The branching program is the analog of the expansion of the determinant by matrix minors.

III. SPIN MODEL

A. Definition and structure

The binary algebraic branching program for the 3×3 permanent [32] suggests a general construction for arbitrary n . Suppose one has a system of spin-1/2 particles, located on sites $j = 0, 1, \dots, n-1$. Each particle can

access states $|0\rangle$ and $|1\rangle$, corresponding to spin down and spin up respectively. The spin model that is the central focus of the current work is defined by the operator

$$\tilde{M} = \sum_{\mathbf{i}} \sum_{j=0}^{n-1} w_{h(\mathbf{i}),j} \sigma_j^+ |\mathbf{i}\rangle \langle \mathbf{i}| + \prod_j \sigma_j^-, \quad (9)$$

where $\sigma_i^+ = |1\rangle\langle 0|_i$ and $\sigma_i^- = |0\rangle\langle 1|_i$ are site-dependent raising and lowering operators. The first sum is over all n -bit strings \mathbf{i} so that a complete and orthonormal basis of n -spin states with dimension 2^n is represented by the unit vectors $|\mathbf{i}\rangle = |\{0,1\}\rangle^{\otimes n}$. The Hamming weight of the bitstring is denoted by $h(\mathbf{i})$, coinciding with the total n -particle spin. Evidently the last term in Eq. (9) is equivalent to $|\mathbf{0}\rangle\langle \mathbf{1}|$.

The operator \tilde{M} defined by Eq. (9) corresponds to the adjacency matrix for a weighted directed graph that effects transitions from the $|\mathbf{0}\rangle$ state to the $|\mathbf{1}\rangle$ state via all possible single-spin raising operations, and then back to $|\mathbf{0}\rangle$ again to complete one cycle. The transition amplitudes are indexed by two integers: the total Hamming weight of the initial state and the target site. With $\sigma_i^+ |1\rangle = 0$, the second index can never be repeated as the value of first index increases; thus, the first term in \tilde{M} encodes all possible transitions from $|\mathbf{0}\rangle$ to $|\mathbf{1}\rangle$ without repetitions. Fig. 2(a) depicts \tilde{M} for $n = 3$, and includes the vertex / state labelings for clarity. The orientation is chosen so that each horizontal layer of the hypercube contains vertices labeled by bitstrings with the same Hamming weight h .

As discussed in detail in what follows, it is convenient to define an alternate encoding of the cyclic behavior of \tilde{M} by eliminating the transition $|\mathbf{0}\rangle\langle \mathbf{1}|$, and instead directly transition from states with Hamming weight $n-1$ to the state $|\mathbf{0}\rangle$. The associated operator is

$$\check{M} = \sum_{\mathbf{i}}' \sum_{j=0}^{n-1} w_{h(\mathbf{i}),j} \sigma_j^+ |\mathbf{i}\rangle \langle \mathbf{i}| + \sum_{j=0}^{n-1} w_{n-1,j} |\mathbf{0}\rangle \langle \mathbf{1}| \sigma_j^+, \quad (10)$$

where the prime on the first term denotes that the sum is over all bitstrings but not including those with Hamming weight $h(\mathbf{i}) = n-1$. In this case, the basis state $|\mathbf{1}\rangle$ is never occupied, and the Hilbert space dimension is reduced to $2^n - 1$. This alternate operator is depicted in Fig. 2(b).

Consider next the $(n+1)$ th (n th) power of \tilde{M} (\check{M}), which will be of central importance in what follows. The derivation is provided in Appendix A, and the result for \tilde{M}^{n+1} is given in Eq. (A5):

$$\begin{aligned} \tilde{M}^{n+1} = & \sum_{j_0, \dots, j_{n-1}} \left[(w_{0,j_0} \sigma_{j_0}^+) \cdots (w_{n-1,j_{n-1}} \sigma_{j_{n-1}}^+) |\mathbf{0}\rangle \langle \mathbf{1}| \right. \\ & + (w_{0,j_0} \sigma_{j_0}^+) \cdots (w_{n-2,j_{n-2}} \sigma_{j_{n-2}}^+) |\mathbf{0}\rangle \langle \mathbf{1}| \\ & \times (w_{n-1,j_{n-1}} \sigma_{j_{n-1}}^+) \\ & + \dots + |\mathbf{0}\rangle \langle \mathbf{1}| (w_{0,j_0} \sigma_{j_0}^+) \cdots (w_{n-1,j_{n-1}} \sigma_{j_{n-1}}^+) \left. \right]. \end{aligned} \quad (11)$$

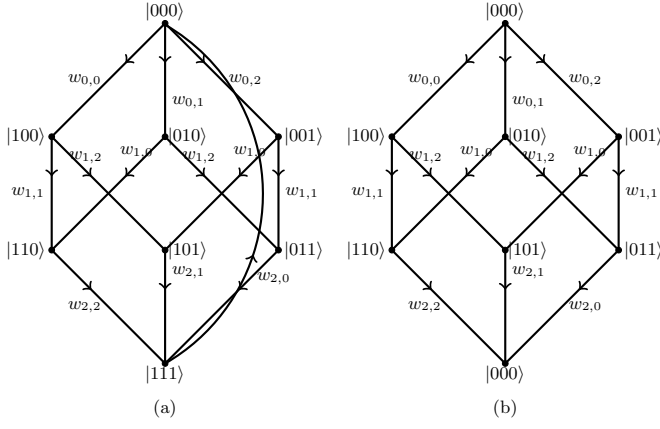


FIG. 2. Depictions of the spin model \tilde{M} (a) and its alternative description \check{M} (b), for $n = 3$.

The expression for $(\check{M})^n$ is identical save for the leading term in Eq. (11).

The above expression can be seen to be of block diagonal form as follows. Each term in the expansion above is defined by the operators $\prod_{r=0}^{m-1} \sigma_{j_r}^+ |\mathbf{0}\rangle\langle\mathbf{1}| \prod_{s=m}^{n-1} \sigma_{j_s}^+$, and is labeled by the index $m = 0, 1, \dots, n$. For $m = 0$, the operator is only $|\mathbf{0}\rangle\langle\mathbf{0}|$, i.e. a block of dimension 1 defined by a single basis state with zero Hamming weight. The $m = 1$ case includes all operators of the form

$$\sigma_{j_0}^+ |\mathbf{0}\rangle\langle\mathbf{1}| \prod_{s=1}^{n-1} \sigma_{j_s}^+ = \sigma_{j_0}^+ |\mathbf{0}\rangle\langle\mathbf{1}| \prod_{s=0}^{n-1} \sigma_{j_s}^+ \sigma_{j_0}^- = \sigma_{j_0}^+ |\mathbf{0}\rangle\langle\mathbf{0}| \sigma_{k_0}^-, \quad (12)$$

which corresponds to a block spanned by the n basis vectors defined by $\sigma_j^+ |\mathbf{0}\rangle$, which are labeled by all bitstrings with unit Hamming weight. Evidently, each block is indexed by the Hamming weight (or total spin) m , and has dimension given by the binomial factor $\binom{n}{m}$. It is convenient to express \tilde{M}^{n+1} as the direct sum

$$\tilde{M}^{n+1} = \tilde{M}_0 \oplus \tilde{M}_1 \oplus \dots \oplus \tilde{M}_n = \bigoplus_{m=0}^n \tilde{M}_m, \quad (13)$$

where \tilde{M}_m corresponds to the block matrix labeled by m and is defined as

$$\tilde{M}_m = \tilde{M}^m |\mathbf{0}\rangle\langle\mathbf{0}| \tilde{M}^{n-m+1}, \quad (14)$$

which has the form

$$\begin{aligned} \tilde{M}_m &= \sum_{j_0, \dots, j_{n-1}} (w_{0,j_0} \sigma_{j_0}^+) (w_{1,j_1} \sigma_{j_1}^+) \dots \\ &\times (w_{m-1,j_{m-1}} \sigma_{j_{m-1}}^+) |\mathbf{0}\rangle\langle\mathbf{1}| (w_{n-1,j_{n-1}} \sigma_{j_{n-1}}^+) \\ &\times (w_{n-2,j_{n-2}} \sigma_{j_{n-2}}^+) \dots (w_{m,j_m} \sigma_{j_m}^+), \end{aligned} \quad (15)$$

as proven as Eq. (A12) in Appendix A. Likewise,

$$\check{M}_m = \check{M}^m |\mathbf{0}\rangle\langle\mathbf{0}| \check{M}^{n-m}. \quad (16)$$

B. Eigensystem

Now turn to the eigenvalues and eigenvectors of the spin model, defined by Eq. (9) or its alternative expression Eq. (10). A key observation is that $|\mathbf{0}\rangle$ is an eigenvector of \tilde{M}^{n+1} or \check{M}^n . Consider the action of \tilde{M}^{n+1} on the state $|\mathbf{0}\rangle$, which only involves the $m = 0$ block:

$$\begin{aligned} \tilde{M}^{n+1} |\mathbf{0}\rangle &= \sum_{j_0, \dots, j_{n-1}} |\mathbf{0}\rangle\langle\mathbf{1}| (w_{0,j_0} w_{1,j_1} \dots w_{n-1,j_{n-1}}) \\ &\times \sigma_{j_0}^+ \sigma_{j_1}^+ \dots \sigma_{j_{n-1}}^+ |\mathbf{0}\rangle. \end{aligned} \quad (17)$$

The action of $\sigma_{j_0}^+ \sigma_{j_1}^+ \dots \sigma_{j_{n-1}}^+$ defines all possible n spin-flip paths from the $|\mathbf{0}\rangle$ state to $|\mathbf{1}\rangle$, and each is weighted by the factor $w_{0,j_0} w_{1,j_1} \dots w_{n-1,j_{n-1}}$. This is precisely the algebraic branching program discussed in Sec. II B; thus

$$\tilde{M}^{n+1} |\mathbf{0}\rangle = \tilde{M}_0 |\mathbf{0}\rangle = P_n |\mathbf{0}\rangle; \quad (18)$$

the eigenvalue is the permanent of M . Likewise, $\check{M}^n |\mathbf{0}\rangle = P_n |\mathbf{0}\rangle$.

The permanent is also an eigenvalue of every other block of \tilde{M}^{n+1} . Defining the block- m state

$$|\psi_m\rangle = \tilde{M}^m |\mathbf{0}\rangle, \quad (19)$$

one obtains

$$\begin{aligned} \tilde{M}_m |\psi_m\rangle &= \tilde{M}^m |\mathbf{0}\rangle\langle\mathbf{0}| \tilde{M}^{n-m+1} \tilde{M}^m |\mathbf{0}\rangle \\ &= \tilde{M}^m |\mathbf{0}\rangle\langle\mathbf{0}| \tilde{M}^{n+1} |\mathbf{0}\rangle = P_n \tilde{M}^m |\mathbf{0}\rangle \\ &= P_n |\psi_m\rangle. \end{aligned} \quad (20)$$

The operator \tilde{M}^{n+1} therefore has $n+1$ degenerate eigenvalues corresponding to the permanent, with associated eigenvectors $|\psi_m\rangle = \tilde{M}^m |\mathbf{0}\rangle$. Likewise, the operator \check{M}^n has n degenerate eigenvalues P_n and associated eigenvectors $\check{M}^m |\mathbf{0}\rangle$.

For the rest of the discussion in this section, we assume that $P_n \neq 0$. Because \tilde{M} is a cycle, if λ is an eigenvalue of \tilde{M}^{n+1} , then the eigenvalues λ_j of \tilde{M} must include all $(n+1)$ th roots of λ (see for example Ref. 33). For the present case $\lambda = P_n$, one obtains $\lambda_j = P_n^{1/(n+1)} e^{-i2\pi j/(n+1)}$, $j = 0, 1, \dots, n$; likewise, the eigenvalues of \check{M} are $(P_n e^{-i2\pi j})^{1/n}$, $j = 0, 1, \dots, n-1$. Given that \check{M} has degeneracy n and therefore only requires n powers to return the state $|\mathbf{0}\rangle$ to itself, it is slightly more convenient to work with \check{M} in what follows.

The eigenvectors of \check{M} with eigenvalues corresponding to the n th roots of P_n can be written as

$$|\phi_n(k)\rangle = e^{-i2\pi k/n} \sum_{j=0}^{n-1} e^{i2\pi jk/n} \left(\frac{\check{M}}{P_n^{1/n}} \right)^j |0^{\otimes n}\rangle, \quad (21)$$

where $k, j = 0, 1, \dots, n-1$. The corresponding eigenval-

ues can be found directly:

$$\begin{aligned}
\check{M}|\phi_n(k)\rangle &= e^{-i2\pi k/n} \sum_{j=0}^{n-1} e^{i2\pi jk/n} P_n^{1/n} \left(\frac{\check{M}}{P_n^{1/n}} \right)^{j+1} |0^{\otimes n}\rangle \\
&= e^{-i4\pi k/n} P_n^{1/n} \sum_{j=0}^{n-1} e^{i2\pi(j+1)k/n} \left(\frac{\check{M}}{P_n^{1/n}} \right)^{j+1} |0^{\otimes n}\rangle \\
&= e^{-i4\pi k/n} P_n^{1/n} \sum_{j=1}^n e^{i2\pi jk/n} \left(\frac{\check{M}}{P_n^{1/n}} \right)^j |0^{\otimes n}\rangle \\
&= e^{-i4\pi k/n} P_n^{1/n} \sum_{j=0}^{n-1} e^{i2\pi jk/n} \left(\frac{\check{M}}{P_n^{1/n}} \right)^j |0^{\otimes n}\rangle \\
&\quad + |0^{\otimes n}\rangle - |0^{\otimes n}\rangle \\
&= e^{-i2\pi k/n} P_n^{1/n} |\phi_n(k)\rangle.
\end{aligned} \tag{22}$$

The eigenvalues are therefore

$$\lambda_k(\check{M}) = e^{-i2\pi k/n} P_n^{1/n} = (e^{-i2\pi k} P_n)^{1/n}. \tag{23}$$

The derivation proceeds analogously for \tilde{M} , and one obtains

$$\lambda_k(\tilde{M}) = (e^{-i2\pi k} P_n)^{1/(n+1)}. \tag{24}$$

The simplest case corresponds to $k = 0$:

$$|\phi_n(0)\rangle = \sum_{j=0}^{n-1} \left(\frac{\check{M}}{P_n^{1/n}} \right)^j |0^{\otimes n}\rangle, \tag{25}$$

with eigenvalue $\lambda_0 = P_n^{1/n}$. Consequently, $\pm\lambda_0$ would be the only real eigenvalues if the elements of M were real and positive. Remarkably, Eq. (23) and (24) constitute the only non-zero eigenvalues of \check{M} and \tilde{M} , respectively.

The periodic nature of \check{M} and \tilde{M} gives rise to eigenvectors that are expanded in a Fourier-like series, much like in a translationally invariant system. In Eq. (21) and Eq. (23), the indices j and k label ‘position’ and ‘wavevector’, respectively. In the present case, the position is the index of the block, corresponding to the Hamming weight or total spin, while the ‘wavevector’ serves essentially the same purpose as in uniform systems: as a canonically conjugate quantum number. Conceptually, one can consider successive applications of \check{M} or \tilde{M} as moving a walker from ‘site’ $|0\rangle$ to ‘site’ $\check{M}|0\rangle$ or $\tilde{M}|0\rangle$, etc., one step (bit flip) at a time, with all states sharing a given Hamming weight treated as equivalent, until it again reaches its starting state (see also Fig. 2).

Given that the determination of the matrix permanent corresponds to an algebraic branching program from the state $|0\rangle$ to itself, effecting the spin transitions in the opposite direction (i.e. reversing the arrows in Fig. 2) corresponds to taking the adjoint (complex conjugate transpose) of \check{M} or \tilde{M} . Eq. (18) then becomes

$$(\check{M}^\dagger)^{n+1} |0\rangle = (\check{M}^\dagger)^n |0\rangle = P_n^* |0\rangle. \tag{26}$$

One can then construct Hermitian operators

$$\tilde{M}_R = \tilde{M}^{n+1} + (\check{M}^\dagger)^{n+1}, \tag{27}$$

$$\tilde{M}_I = i \left[\tilde{M}^{n+1} - (\check{M}^\dagger)^{n+1} \right], \tag{28}$$

satisfying the eigenvalue equations

$$\tilde{M}_R |0\rangle = \text{Re}(P_n) |0\rangle; \tag{29}$$

$$\tilde{M}_I |0\rangle = \text{Im}(P_n) |0\rangle. \tag{30}$$

Similar expressions apply to \check{M} . While the operators (27) and (28) are arguably more physical, their experimental realization could remain challenging given the complexity of the description, Eq. (11). Also, unlike the case for \tilde{M}^{n+1} or \check{M}^n alone, the non-zero eigenvalues for the remaining blocks of (27) and (28) are different from $\text{Re}(P_n)$ and $\text{Im}(P_n)$.

C. Classical Algorithm for the permanent

While the result (18) is a statement about the eigenvalues, it suggests a straightforward approach to the calculation of the permanent without needing to determine the spectrum of \tilde{M} or \check{M} . Rather, one must only compute

$$\tilde{M}^n |0\rangle = P_n |1\rangle \text{ or } \tilde{M}^{n+1} |0\rangle = P_n |0\rangle; \text{ or } \check{M}^n |0\rangle = P_n |0\rangle. \tag{31}$$

In other words, apply \tilde{M} or \check{M} successively to the state $|0\rangle$ until all the amplitude is again concentrated on the state $|0\rangle$, and read out the result.

The algorithm for the permanent then corresponds to an n -fold or $(n-1)$ -fold product of matrices with dimension $\binom{n}{i+1} \times \binom{n}{i}$ ($i = \{0, 1, \dots, n-1\}$). Each column of the i th matrix contains exactly $n-i$ non-zero elements, so that the matrices are exponentially sparse. The total number of operations (multiplications and additions) is

$$\sum_{i=1}^n \binom{n}{i} (2i) = n2^n. \tag{32}$$

In comparison, Ryser’s algorithm requires a total of $n2^{n+1} - (n+1)^2 \sim 2n2^n$ operations for large n [15]. The scaling of the number of operations in the present case therefore matches that of the fastest-known algorithm, with a straightforward implementation, which could make it useful for practical applications.

IV. FERMIONIC AND BOSONIC REPRESENTATIONS

The spin model (9) can be naturally represented in terms of Schwinger bosons, and fermions via the Jordan-Wigner transformation. These are discussed in the next two subsections.

A. Bosons

Spin-1/2 particles can be mapped to Schwinger bosons as follows:

$$\begin{aligned}\sigma_j^+ &= \sigma_j^x - i\sigma_j^y = a_j^\dagger b_j; \\ \sigma_j^- &= \sigma_j^x + i\sigma_j^y = b_j^\dagger a_j; \\ \sigma_j^z &= a_j^\dagger a_j - b_j^\dagger b_j.\end{aligned}\quad (33)$$

Each spin operator therefore involves two ‘species’ of bosons, satisfying the relations

$$[a_i, a_j^\dagger] = \delta_{ij}; \quad [a_i, a_j] = [a_i^\dagger, a_j^\dagger] = 0 \quad (34)$$

and likewise for b -species bosons, where $[x, y] = xy - yx$ is the commutator. These are supplemented with the unit-occupancy condition

$$a_j^\dagger a_j + b_j^\dagger b_j = 1, \quad (35)$$

which specifies that each site is occupied by exactly one boson of either species. The Schwinger approach therefore maps spins to hard-core two-species bosons at exactly unit filling. The model (9) expressed in terms of Schwinger bosons is then

$$\tilde{M}_b = \sum_{\mathbf{i}} \sum_{j=0}^{n-1} w_{h(\mathbf{i}),j} a_j^\dagger b_j |\mathbf{i}\rangle \langle \mathbf{i}| + \prod_j b_j^\dagger a_j, \quad (36)$$

where the bit in the string \mathbf{i} is unity (zero) if occupied by a boson of species a (b), and the zero state is

$$|\mathbf{0}\rangle = \prod_{j=0}^{n-1} b_j^\dagger |\mathcal{O}\rangle. \quad (37)$$

The graph associated with \tilde{M}_b is indistinguishable from that of \tilde{M} , i.e. Fig. 2 for $n = 3$.

It is instructive to write the action of the n th power of \tilde{M}_b on the zero state:

$$\begin{aligned}\tilde{M}_b^n |\mathbf{0}\rangle &= \left(\sum_{j=0}^{n-1} w_{n-1,j} a_j^\dagger b_j \right) \left(\sum_{j=0}^{n-1} w_{n-2,j} a_j^\dagger b_j \right) \\ &\times \cdots \times \left(\sum_{j=0}^{n-1} w_{0,j} a_j^\dagger b_j \right) \prod_{j=0}^{n-1} b_j^\dagger |\mathcal{O}\rangle \\ &= \left(\sum_{j=0}^{n-1} w_{n-1,j} a_j^\dagger \right) \left(\sum_{j=0}^{n-1} w_{n-2,j} a_j^\dagger \right) \\ &\times \cdots \times \left(\sum_{j=0}^{n-1} w_{0,j} a_j^\dagger \right) |\mathcal{O}\rangle.\end{aligned}\quad (38)$$

In the second line above, all operators for the b -species bosons can be omitted because each creation of an a -species boson must be accompanied by the annihilation of

a b -species boson, and after n powers of \tilde{M}_b all sites have been accounted for. Furthermore, the hard-core condition acts in the same way as a Pauli exclusion principle: if a b -species boson occupies site j , then the b_j^\dagger operator returns zero. Expansion of the terms in Eq. (38) then returns the permanent because the b -species bosons all commute.

B. Fermions

The Jordan-Wigner transformation corresponds to mapping the spin operators to ‘spinless’ fermions:

$$\begin{aligned}\sigma_j^+ &= \exp \left(i\pi \sum_{k=j+1}^{n-1} f_k^\dagger f_k \right) f_j^\dagger; \\ \sigma_j^- &= \exp \left(i\pi \sum_{k=j+1}^{n-1} f_k^\dagger f_k \right) f_j; \\ \sigma_j^z &= 2f_j^\dagger f_j - 1,\end{aligned}\quad (39)$$

where the site-dependent fermionic creation (f_j^\dagger) and annihilation (f_j) operators satisfy the anticommutation relations

$$\{f_i, f_j^\dagger\} = \delta_{ij}; \quad \{f_i, f_j\} = \{f_i^\dagger, f_j^\dagger\} = 0, \quad (40)$$

and $\{x, y\} = xy + yx$. The first of these automatically ensures the Pauli condition forbidding double occupancy of sites; thus, basis states can therefore again be indexed by bitstrings \mathbf{i} , but now where 0 (1) signifies the absence (presence) of a fermion at position j . Canonical ordering is assumed, where creation operators appear with indices in descending order; for example

$$|1010\rangle = f_2^\dagger f_0^\dagger |\mathcal{O}\rangle, \quad (41)$$

where $|\mathcal{O}\rangle$ denotes the particle vacuum.

The phases appearing in Eq. (39) ensure that the fermions anticommute on all sites; alternatively, they ensure the normal / canonical ordering of basis states. For example:

$$\begin{aligned}f_0^\dagger |1010\rangle &= f_0^\dagger f_2^\dagger f_0^\dagger |\mathcal{O}\rangle = 0; \\ f_1^\dagger |1010\rangle &= f_1^\dagger f_2^\dagger f_0^\dagger |\mathcal{O}\rangle = -f_2^\dagger f_1^\dagger f_0^\dagger |\mathcal{O}\rangle = -|1110\rangle; \\ f_3^\dagger |1010\rangle &= f_3^\dagger f_2^\dagger f_0^\dagger |\mathcal{O}\rangle = |1011\rangle.\end{aligned}\quad (42)$$

The Jordan-Wigner transformation (39) counts the number of fermions to the right of (i.e. with index greater than) where the spin is flipped / fermion is created, and multiplies the transition amplitude by -1 if this number is odd. In this way, the negative signs arising from the fermionic anticommutation are cancelled and the transition amplitudes all remain positive. The model (9) expressed in terms of fermions then becomes

$$\tilde{M}_{\text{JW}} = \sum_{\mathbf{i}} \sum_{j=0}^{n-1} w_{h(\mathbf{i}),j} s_{\mathbf{i},j} f_j^\dagger |\mathbf{i}\rangle \langle \mathbf{i}| + \prod_j f_j, \quad (43)$$

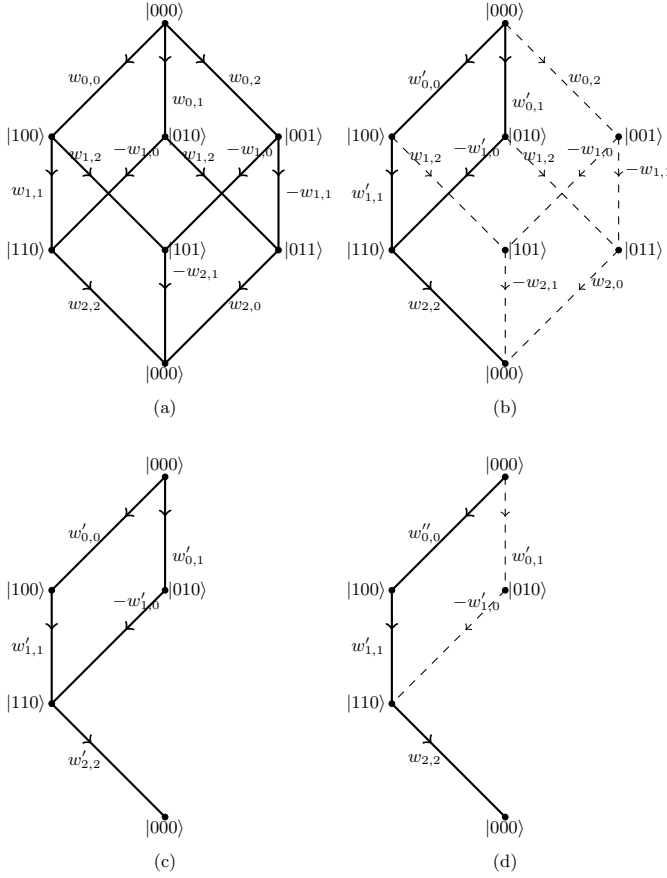


FIG. 3. Depictions of the fermionic model $\tilde{M}_{f,\text{alt}}$, Eq. (45) with $|111\rangle \rightarrow |000\rangle$, for $n = 3$. Its original form is shown in (a), while various stages of row reduction are shown in (b)-(d).

where the function $s_{i,j}$ incorporates the Jordan-Wigner phases for creation of a fermion at position j on a basis state with occupation indexed by occupation state $|\mathbf{i}\rangle$ defined by bitstring \mathbf{i} .

An explicit example is shown for the $n = 3$ case in Fig. 3(a). Consider the $|100\rangle \rightarrow |110\rangle$ and $|010\rangle \rightarrow |110\rangle$ transitions. For the former transition, a fermion is created in site 1, to the right of a fermion already in site 0, so there is no additional Jordan-Wigner phase; likewise, the final state $|110\rangle = f_1^\dagger f_0^\dagger |\mathcal{O}\rangle$ is already normal ordered. Thus, the edge weight $w_{1,1}$ remains unchanged. For the latter transition, the fermion created in site 0 is to the left of a fermion already in site 1, which yields a negative contribution from the Jordan-Wigner transformation, reflected in the signed edge weight $-w_{1,0}$ in Fig. 3(a). At the same time, the final state $|110\rangle = f_0^\dagger f_1^\dagger |\mathcal{O}\rangle$ requires one fermionic anticommutation to bring it back to normal ordering, which cancels the negative sign and effectively restores the total edge weight to its original value in the spin representation. Thus, within the context of a binary branching process, the sum of the path weights of Fig. 3(a) still constitute the permanent, despite the

appearance of signed edge weights.

To construct an algebraic branching program for true fermions one either must maintain all edge weights and keep track of the fermionic anticommutation relations defining the occupation states, in which case the model is

$$\tilde{M}_f = \sum_{\mathbf{i}} \sum_{j=0}^{n-1} w_{h(\mathbf{i}),j} f_j^\dagger |\mathbf{i}\rangle \langle \mathbf{i}| + \prod_j f_j \quad (44)$$

and $|\mathbf{i}\rangle$ represent occupation states; or one must account for all Jordan-Wigner phases to appropriately sign all edge weights but treat the states $|\mathbf{i}\rangle$ instead as ordinary bitstrings, in which case the model is instead

$$\tilde{M}_{f,\text{alt}} = \sum_{\mathbf{i}} \sum_{j=0}^{n-1} w_{h(\mathbf{i}),j} s_{\mathbf{i},j} \sigma_j^+ |\mathbf{i}\rangle \langle \mathbf{i}| + \prod_j \sigma_j^-, \quad (45)$$

and now the σ^\pm are interpreted as classical bit-flip operators. When expressing the fermionic model in terms of creation and annihilation operators, Eq. (44) is preferable, but Eq. (45) is more convenient in the graph adjacency matrix representation. Now, Fig. 3(a) depicts a truly signed binary branching process, and the sum of the path weights constitute the determinant, rather than the permanent, of M for $n = 3$. The $w_{0,0}w_{1,1}w_{2,2}$ path serves as the reference, where the second indices for the weights in this product constitute the integer list $\{012\}$. All other paths are characterized by an overall minus (plus) sign if the integer list derived from the second index of the weights for that path corresponds to an even (odd) number of inversions of the reference list; for example, the odd permutations $\{021\}$, $\{102\}$, and $\{210\}$ correspond to paths with negative total weights $-w_{0,0}w_{1,2}w_{2,1}$, $-w_{0,1}w_{1,0}w_{2,2}$, and $-w_{0,2}w_{1,1}w_{2,0}$, respectively. Thus, one expects that the eigenvalues of the operator (44) are the determinant, as will be discussed further below.

Another noteworthy property of the fermionic graph is that it is unbalanced: there is no vertex sign switching that can remove all of the minus signs [34]; alternatively expressed, there is no diagonal matrix whose entries are $\{1, -1\}$ that can map Eq. (44) to a form without any $s_{i,j}$ factors. (This is another way of stating that the determinant derived in this way cannot be mapped to the permanent by a local unitary, though this is already obvious as unitary transformations preserve the eigenvalues). There remains the intriguing possibility that there is a non-unitary operator that can effect the map, but this is not explored in the present work.

Similarly, it is not possible to map existing weights to their negatives in order to map the determinant to the permanent. For the $n = 3$ case, one could reassign $w_{1,2} \rightarrow -w_{1,2}$ and $w_{2,1} \rightarrow -w_{2,1}$ to remove the negative signs on all edges with these labels in Fig. 3(a), but this still leaves signs on edges labeled by $w_{1,1}$ which cannot be removed.

As in the bosonic case, it is worthwhile to express the action of the n th power of $\tilde{M}_{f,\text{alt}}$ on the vacuum state:

$$\begin{aligned} \tilde{M}_f^n |\mathbf{0}\rangle &= \left(\sum_{j=0}^{n-1} w_{n-1,j} f_j^\dagger \right) \left(\sum_{j=0}^{n-1} w_{n-2,j} f_j^\dagger \right) \\ &\times \cdots \times \left(\sum_{j=0}^{n-1} w_{0,j} f_j^\dagger \right) |\mathcal{O}\rangle. \end{aligned} \quad (46)$$

This simple and apparently separable representation for the output state, as products of similar terms, is possible because of the Pauli principle and the anticommutation relations: any attempted creation of a fermion in an already-occupied site is zero, and the signs of the final many-fermion states will reflect the number of permutations required to express them in normal ordering. Furthermore, the result is clearly the determinant D_n (or its negative) rather than the permanent. The states (46) and (38) reveal a close connection between the determinant and the permanent expressed in terms of indistinguishable particles.

Consider explicitly the $n = 3$ case:

$$\begin{aligned} \tilde{M}_f^3 |\mathbf{0}\rangle &= (w_{2,0} f_0^\dagger + w_{2,1} f_1^\dagger + w_{2,2} f_2^\dagger) \\ &\times (w_{1,0} f_0^\dagger + w_{1,1} f_1^\dagger + w_{1,2} f_2^\dagger) \\ &\times (w_{0,0} f_0^\dagger + w_{0,1} f_1^\dagger + w_{0,2} f_2^\dagger) |\mathcal{O}\rangle \\ &= w_{2,2} f_2^\dagger (w_{1,1} f_1^\dagger w_{0,0} f_0^\dagger + w_{1,0} f_0^\dagger w_{0,1} f_1^\dagger) \\ &+ w_{2,1} f_1^\dagger (w_{1,2} f_2^\dagger w_{0,0} f_0^\dagger + w_{1,0} f_0^\dagger w_{0,2} f_2^\dagger) \\ &+ w_{2,0} f_0^\dagger (w_{1,1} f_1^\dagger w_{0,2} f_2^\dagger + w_{1,2} f_2^\dagger w_{0,1} f_1^\dagger) |\mathcal{O}\rangle \\ &= [w_{2,2} (w_{1,1} w_{0,0} - w_{1,0} w_{0,1}) \\ &+ w_{2,1} (-w_{1,2} w_{0,0} + w_{1,0} w_{0,2}) \\ &+ w_{2,0} (-w_{1,1} w_{0,2} + w_{1,2} w_{0,1})] f_2^\dagger f_1^\dagger f_0^\dagger |\mathcal{O}\rangle \\ &= D_3 f_2^\dagger f_1^\dagger f_0^\dagger |\mathcal{O}\rangle. \end{aligned} \quad (47)$$

Recapitulating the arguments of Sec. IIIB but for \tilde{M}_f instead of \tilde{M} or \check{M} , one obtains that the only non-zero eigenvalues of \tilde{M}_f are given by the $(n+1)$ th roots of D_n .

V. ROW REDUCTIONS

The exponentially small rank of the matrices \tilde{M} and \check{M} , discussed in Section IIIB, suggests that it might be possible to apply row reductions to reduce their dimension without affecting the non-zero eigenvalues. Just as Gaussian elimination reduces a matrix to upper (or lower) triangular form, so that the determinant (which would otherwise require summing $n!$ terms) can be evaluated by a product of the diagonal elements, row reduction of \tilde{M} or \check{M} reduces the $n!$ paths of the algebraic branching program to a single path by deleting vertices

and reweighting edges. As shown below, row reductions in the fermionic model correspond precisely to the Gaussian elimination approach to evaluating the determinant. The bosonic version provides a roadmap for row reductions to evaluate the permanent, but doesn't appear to provide a speedup over the direct matrix multiplication method discussed in Sec. IIIC.

As shown in Sec. IIIB, the blocks \tilde{M}_m of \tilde{M}^{n+1} and \check{M}^n have dimension $\binom{n}{m}$ but are all unit rank, so that the ranks of \tilde{M}^{n+1} and \check{M}^n are $n+1$ and n , respectively. In contrast, the matrices \tilde{M} and \check{M} are not block diagonal, and their eigenvectors are no longer given by $\tilde{M}^m |\mathbf{0}\rangle$ and $\check{M}^m |\mathbf{0}\rangle$, respectively. Consider \check{M} for concreteness. While the n non-zero eigenvalues correspond to the n th roots of the permanent, the zero eigenvalues have multiplicity $2^n - n$; thus, the kernel of \check{M} is comprised of generalized zero eigenvectors of rank 1 up to $n-1$. The set of linearly independent vectors spanning these defective matrices must therefore be obtained sequentially. The standard procedure is to obtain the set of r_m generalized zero rank- m vectors $|v_i^{(m)}\rangle$, $1 \leq i \leq r_m$, such that $\check{M}^m |v_i^{(m)}\rangle = |\mathcal{O}\rangle$. The rank-nullity theorem ensures that $n + \sum_{m=1}^{n-1} r_m = 2^n - 1$.

In practice there is a more efficient iterative procedure to obtain the kernel. First generate the reduced row echelon form (also known as the pivot matrix) B_1 for \check{M} , via Gauss-Jordan elimination. For any rank-deficient matrix such as \check{M} , the deviation of B_1 from the identity is driven entirely by the r_1 rank-1 zero eigenvectors; thus the $(2^n - 1 - r_1) \times (2^n - 1)$ matrix B_1 annihilates the null space: $B_1 |v_i^{(1)}\rangle = 0$. One can then find an $n \times (2^n - 1 - r_1)$ matrix A_1 such that $\check{M} = A_1 B_1$; its matrix elements coincide with those of \check{M} but with r_1 columns removed whose indices correspond to the location of the first non-zero element of each $|v_i^{(1)}\rangle$. The $(2^n - 1 - r_1) \times (2^n - 1 - r_1)$ matrix $\check{M}^{(2)} \equiv B_1 A_1$ therefore has the same eigenvalues as \check{M} but now with r_1 fewer zeroes.

The rank-2 generalized eigenvectors are the solutions of

$$\check{M}^2 |v_i^{(2)}\rangle = A_1 B_1 A_1 B_1 |v_i^{(2)}\rangle = |\mathcal{O}\rangle, \quad (48)$$

for $1 \leq i \leq r_2$, which can be rewritten as

$$A_1 \check{M}^{(2)} (B_1 |v_i^{(2)}\rangle) = 0. \quad (49)$$

At the same time, the zero eigenvectors of $\check{M}^{(2)}$ are the solutions of

$$\check{M}^{(2)} |\tilde{v}_i^{(2)}\rangle = 0. \quad (50)$$

Thus, with the identification $|\tilde{v}_i^{(2)}\rangle \equiv B_1 |v_i^{(2)}\rangle$, Eq. (49) is automatically satisfied by Eq. (50), and solving the latter is more efficient than the former due to the smaller matrix dimension. It is straightforward to verify that the non-zero eigenstates of interest from Eq. (21),

$$|\phi_n^{(1)}(k)\rangle = e^{-i2\pi k/n} \sum_{j=0}^{n-1} e^{i2\pi jk/n} \left(\frac{\check{M}}{P_n^{1/n}} \right)^j |\mathbf{0}^{\otimes n}\rangle, \quad (51)$$

are transformed into

$$\begin{aligned} |\phi_n^{(2)}(k)\rangle &= e^{-i2\pi k/n} \sum_{j=0}^{n-1} e^{i2\pi jk/n} \left(\frac{\check{M}^{(2)}}{P_n^{1/n}} \right)^j |0^{\otimes n}\rangle \\ &= B_1 |\phi_n^{(1)}(k)\rangle. \end{aligned} \quad (52)$$

The procedure is then repeated for $\check{M}^{(2)} = A_2 B_2$. After $n - 1$ iterations, the original rank-deficient $(2^n - 1)$ -dimensional matrix \check{M} is reduced to a full-rank n -dimensional matrix $\check{M}^{(n-1)}$ with eigenvectors $\prod_{i=1}^{n-1} B_{n-i} |\phi_n(k)\rangle$ and corresponding eigenvalues $P_n^{1/n}$. As shown below, this procedure is equivalent to Gaussian elimination of M for the evaluation of the determinant, and also provides an equivalent systematic approach to the evaluation of the permanent.

A. Example: Three Fermions

Consider row reductions of $\check{M}_{f,\text{alt}}$, Eq. (45), for the specific case $n = 3$, depicted in Fig. 3). The (unnormalized) rank-1 generalized zero eigenvectors can be written as

$$\begin{aligned} |v_1^{(1)}\rangle &= |001\rangle + \frac{w_{1,1}}{w_{1,2}} |010\rangle + \frac{w_{1,0}}{w_{1,2}} |100\rangle; \\ |v_2^{(1)}\rangle &= |011\rangle - \frac{w_{2,0}}{w_{2,2}} |110\rangle; \\ |v_3^{(1)}\rangle &= |101\rangle + \frac{w_{2,1}}{w_{2,2}} |110\rangle, \end{aligned} \quad (53)$$

so that one may eliminate vertices labeled by the bitstrings 001, 011, and 101. The matrix B_1 must satisfy $B_1 |v_i^{(1)}\rangle = 0$; a sufficient construction is

$$\begin{aligned} B_1 &= I - |v_1^{(1)}\rangle\langle 001| - |v_2^{(1)}\rangle\langle 011| - |v_3^{(1)}\rangle\langle 101| \\ &= \begin{pmatrix} 1 & 0 & 0 & 0 & 0 & 0 & 0 \\ 0 & -\frac{w_{1,1}}{w_{1,2}} & 1 & 0 & 0 & 0 & 0 \\ 0 & -\frac{w_{1,0}}{w_{1,2}} & 0 & 0 & 1 & 0 & 0 \\ 0 & 0 & 0 & \frac{w_{2,0}}{w_{2,2}} & 0 & -\frac{w_{2,1}}{w_{2,2}} & 1 \end{pmatrix}, \end{aligned} \quad (54)$$

where rows and columns indices are labeled by bitstrings with the least significant bit on the right. Here, B_1 is expressed in the somewhat unconventional lower-triangular reduced row echelon form. Likewise,

$$\begin{aligned} A_1 &= \check{M}_{f,\text{alt}} \setminus \{ \langle 001|, \langle 011|, \langle 101| \} \\ &= \begin{pmatrix} 0 & 0 & 0 & w_{2,2} \\ w_{0,2} & 0 & 0 & 0 \\ w_{0,1} & 0 & 0 & 0 \\ 0 & w_{1,2} & 0 & 0 \\ w_{0,0} & 0 & 0 & 0 \\ 0 & 0 & w_{1,2} & 0 \\ 0 & -w_{1,0} & w_{1,1} & 0 \end{pmatrix}. \end{aligned} \quad (55)$$

It is straightforward to verify that $A_1 B_1 = \check{M}_{f,\text{alt}}$. One then obtains

$$\check{M}_{f,\text{alt}}^{(2)} = B_1 A_1 = \begin{pmatrix} 0 & 0 & 0 & w_{2,2} \\ w'_{0,1} & 0 & 0 & 0 \\ w'_{0,0} & 0 & 0 & 0 \\ 0 & -w'_{1,0} & w'_{1,1} & 0 \end{pmatrix}, \quad (56)$$

where $w'_{0,0}$, $w'_{0,1}$, $w'_{1,0}$, and $w'_{1,1}$ coincide with the reweighted terms in M derived from a first round of Gaussian elimination, defined in Eqs. (4) and (5).

It is illuminating to view this first round as an operation on the graph representing the binary branching process, as depicted in Figs. 3(b) and (c). Vertices labeled by bitstrings 001, 011, and 101 are deleted, reducing the total number of branches from six to two. The contributions to the determinant of the branches through the deleted vertices are incorporated by reweighting remaining edges. For example, the weight $-w_{1,2}w_{2,1}$ of the path from $|100\rangle$ to $|000\rangle$ through vertex $|101\rangle$ is incorporated into the new path weight $w'_{1,1}w_{2,2}$; similarly, the path from $|010\rangle$ to $|000\rangle$ through deleted vertex $|011\rangle$ is incorporated in $w'_{1,0}$. Perhaps surprisingly, these edge reweightings can also compensate for both of the deleted paths from $|001\rangle$ to $|000\rangle$ through the two deleted vertices $|011\rangle$ and $|101\rangle$. Crucially, for fermions, the total path weights after the transformation are products of revised edge weights; as discussed in Sec. II A, cancellation of signed terms ensure that the total weights for the reduced branching process still coincide with the determinant.

The remaining (unnormalized) rank-2 generalized zero eigenvector can now be efficiently written as

$$|v^{(2)}\rangle = |010\rangle + \frac{w'_{1,0}}{w'_{1,1}} |100\rangle, \quad (57)$$

so that one may eliminate the vertex labeled by the bitstring 010. The matrix B_2 must satisfy $B_2 |v^{(2)}\rangle = |0\rangle$:

$$\begin{aligned} B_2 &= I - |v^{(2)}\rangle\langle 010| \\ &= \begin{pmatrix} 1 & 0 & 0 & 0 \\ 0 & -\frac{w'_{1,0}}{w'_{1,1}} & 1 & 0 \\ 0 & 0 & 0 & 1 \end{pmatrix}. \end{aligned} \quad (58)$$

Likewise,

$$\begin{aligned} A_2 &= \check{M}_{f,\text{alt}}^{(2)} \setminus \{ \langle 010| \} \\ &= \begin{pmatrix} 0 & 0 & w_{2,2} \\ w'_{0,1} & 0 & 0 \\ w'_{0,0} & 0 & 0 \\ 0 & w'_{1,1} & 0 \end{pmatrix}. \end{aligned} \quad (59)$$

Again, it is straightforward to verify that $A_2 B_2 = \check{M}_{f,\text{alt}}^{(2)}$. One then obtains

$$\check{M}_{f,\text{alt}}^{(3)} = B_2 A_2 = \begin{pmatrix} 0 & 0 & w_{2,2} \\ w''_{0,0} & 0 & 0 \\ 0 & w'_{1,1} & 0 \end{pmatrix}, \quad (60)$$

where $w''_{0,0}$ coincides with Eq. (7). The eigenvalues of $\tilde{M}^{(3)}$ are the cube roots of $D_3 = w''_{0,0}w'_{1,1}w_{2,2}$. In this example, the second and final round of Gauss-Jordan elimination corresponds to deleting the vertex labeled by bitstring 010, as depicted in Fig. 3(d), yielding only one path from $|000\rangle$ to $|000\rangle$ and the rescaled weight $w''_{0,0}$. The product of the edge weights for this path, $w''_{0,0}w'_{1,1}w_{2,2}$ is precisely the product of diagonal terms of \tilde{M} in lower-triangular form, Eq. (6).

It is instructive to write the consequences of row reduction for the fermionic representation of the eigenstate, Eq. (47), for the example considered above. After the first round, the state becomes

$$\begin{aligned} \tilde{M}_f^3|0\rangle &= w_{2,2}f_2^\dagger \left(w'_{1,0}f_0^\dagger + w'_{1,1}f_1^\dagger \right) \\ &\times \left(w'_{0,0}f_0^\dagger + w'_{0,1}f_1^\dagger \right) |\mathcal{O}\rangle, \end{aligned} \quad (61)$$

using the Pauli principle. After the second round, one obtains

$$\tilde{M}_f^3|0\rangle = w_{2,2}f_2^\dagger w'_{1,1}f_1^\dagger w''_{0,0}f_0^\dagger |\mathcal{O}\rangle = D_3 f_2^\dagger f_1^\dagger f_0^\dagger |\mathcal{O}\rangle. \quad (62)$$

Thus, for fermions, no explicit expansion of the state (47) is required; rather, the initial product of factors with three terms is reduced to a product of factors with two terms, and finally a product of single terms. The general strategy is the same for all n . This reduction of the evaluation of the determinant to a product of n terms is at the heart of its efficiency.

B. Example: Three Bosons

Consider next row reductions for the bosonic case, again using $n = 3$ as an example to illustrate the procedure for general n . The procedure works in much the same way as for fermions, and is depicted in Fig. 4). The initial graph is equivalent to that for the original spin model, and is shown in Fig. 2).

The (unnormalized) rank-1 generalized zero eigenvectors of \tilde{M}_b , Eq. (10), can be written as

$$\begin{aligned} |v_1^{(1)}\rangle &= |011\rangle - \frac{w_{2,0}}{w_{2,2}}|110\rangle; \\ |v_2^{(1)}\rangle &= |101\rangle - \frac{w_{2,1}}{w_{2,2}}|110\rangle. \end{aligned} \quad (63)$$

Comparison with Eq. (53), one notices the similarity with $|v_2^{(1)}\rangle$ and $|v_3^{(1)}\rangle$ in the fermionic case, and also that there is no rank-1 zero eigenvector involving $h = 1$ states. The vertices labeled by the bitstrings 011 and 101 can be eliminated choosing the projector

$$\begin{aligned} B_1 &= I - |v_1^{(1)}\rangle\langle 011| - |v_2^{(1)}\rangle\langle 101| \\ &= \begin{pmatrix} 1 & 0 & 0 & 0 & 0 & 0 \\ 0 & 1 & 0 & 0 & 0 & 0 \\ 0 & 0 & 1 & 0 & 0 & 0 \\ 0 & 0 & 0 & 0 & 1 & 0 \\ 0 & 0 & 0 & \frac{w_{2,0}}{w_{2,2}} & 0 & \frac{w_{2,1}}{w_{2,2}} \\ 0 & 0 & 0 & 0 & 0 & 1 \end{pmatrix}, \end{aligned} \quad (64)$$

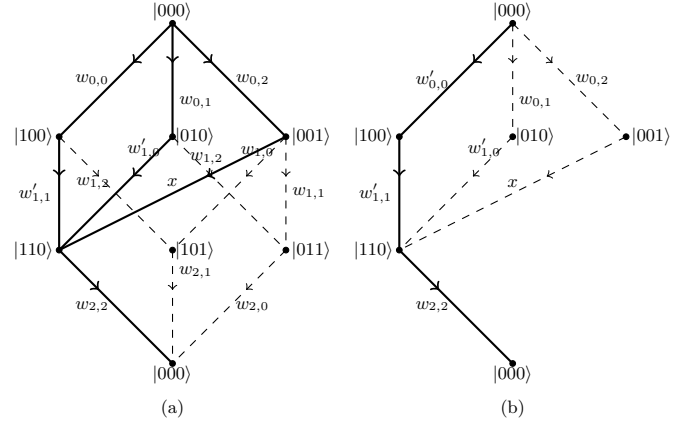


FIG. 4. Round 1 (a) and 2 (b) of row reduction for the original spin model, equivalent to Schwinger bosons, for $n = 3$.

and

$$\begin{aligned} A_1 &= \tilde{M}_b \setminus \{ \langle 011|, \langle 101| \} \\ &= \begin{pmatrix} 0 & 0 & 0 & 0 & w_{2,2} \\ w_{0,2} & 0 & 0 & 0 & 0 \\ w_{0,1} & 0 & 0 & 0 & 0 \\ 0 & w_{1,1} & w_{1,2} & 0 & 0 \\ w_{0,0} & 0 & 0 & 0 & 0 \\ 0 & w_{1,0} & 0 & w_{1,2} & 0 \\ 0 & 0 & w_{1,0} & w_{1,1} & 0 \end{pmatrix}. \end{aligned} \quad (65)$$

Again, it is straightforward to verify that $A_1 B_1 = \tilde{M}$. One then obtains

$$\tilde{M}^{(2)} = B_1 A_1 = \begin{pmatrix} 0 & 0 & 0 & 0 & w_{2,2} \\ w_{0,2} & 0 & 0 & 0 & 0 \\ w_{0,1} & 0 & 0 & 0 & 0 \\ w_{0,0} & 0 & 0 & 0 & 0 \\ 0 & x & w'_{1,0} & w'_{1,1} & 0 \end{pmatrix}, \quad (66)$$

where $w'_{1,0}$, and $w'_{1,1}$ coincide with the expressions in Eq. (5) but with minus signs replaced with plus signs; and a new term is introduced,

$$x = \frac{w_{1,0}w_{2,1} + w_{1,1}w_{2,0}}{w_{2,2}}. \quad (67)$$

The first round of row reductions, shown in Fig. 4(a), corresponds to deleting two vertices in the $h = 2$ layer but none in the $h = 1$ layer, in contrast with the fermionic case. Deleting vertices in only a single layer avoids generating paths with rescaled weights on two adjacent edges, which would yield unphysical cross terms in their product (c.f. the discussion in Sec. II A). But this comes at a high cost: vertices cannot be deleted in an adjacent layer simultaneously if they share edges with vertices in the first layer, as is possible in the fermionic case. This clearly decreases the efficiency of the reduction. Furthermore, deleting vertices in one layer requires adding new edges from the remaining vertex in that layer to all vertices in the next layer that had (now deleted) edges; in this case, the additional edge has weight x .

The second and final round of row reductions in this example is governed by the rank-2 generalized zero eigenvectors:

$$\begin{aligned} |v_1^{(2)}\rangle &= |001\rangle - \frac{x}{w'_{1,1}}|100\rangle; \\ |v_2^{(2)}\rangle &= |010\rangle - \frac{w'_{1,0}}{w'_{1,1}}|100\rangle. \end{aligned} \quad (68)$$

As shown in Fig. 4(b), the vertices labeled by the bit-strings 001 and 010 are eliminated:

$$\begin{aligned} B_2 &= I - |v_1^{(2)}\rangle\langle 001| - |v_2^{(2)}\rangle\langle 010| \\ &= \begin{pmatrix} 1 & 0 & 0 & 0 & 0 \\ 0 & \frac{x}{w'_{1,1}} & \frac{w'_{1,0}}{w'_{1,1}} & 1 & 0 \\ 0 & 0 & 0 & 0 & 1 \end{pmatrix}, \end{aligned} \quad (69)$$

and

$$\begin{aligned} A_2 &= \check{M}^{(2)} \setminus \{\langle 001|, \langle 010|\} \\ &= \begin{pmatrix} 0 & 0 & w_{2,2} \\ w_{0,2} & 0 & 0 \\ w_{0,1} & 0 & 0 \\ w_{0,0} & 0 & 0 \\ 0 & w'_{1,1} & 0 \end{pmatrix}. \end{aligned} \quad (70)$$

One then obtains

$$\tilde{M}^{(3)} = B_2 A_2 = \begin{pmatrix} 0 & 0 & w_{2,2} \\ w'_{0,0} & 0 & 0 \\ 0 & w'_{1,1} & 0 \end{pmatrix}, \quad (71)$$

where

$$w'_{0,0} = w_{0,0} + \frac{w_{0,1}w'_{1,0} + w_{0,2}x}{w'_{1,1}}. \quad (72)$$

As is shown in Fig. 4(b), two vertices in the $h = 1$ layer are now deleted, requiring a rescaling of the $w_{0,0}$ weight, and one obtains a single path from $|000\rangle$ to $|000\rangle$, as desired. The permanent is then

$$P_3 = w'_{0,0}w'_{1,1}w_{2,2}, \quad (73)$$

which is expressed as a product of three single terms, much like the expression of the determinant in Eq. (2).

C. Example: Four Bosons

Given the superficial similarities between row reductions for the bosonic and fermionic cases when $n = 3$, it is instructive to discuss the $n = 4$ case to gather a better understanding of why the permanent is nevertheless exponentially more difficult to compute with this method.

The rank-1 generalized zero eigenvectors are

$$\begin{aligned} |v_1^{(1)}\rangle &= |0011\rangle - \frac{w_{2,1}}{w_{2,3}}|0110\rangle - \frac{w_{2,0}}{w_{2,2}}|1001\rangle + \frac{w_{2,0}w_{2,1}}{w_{2,2}w_{2,3}} \\ &= \left(|01\rangle - \frac{w_{2,0}}{w_{2,2}}|10\rangle\right)_{0,2} \left(|01\rangle - \frac{w_{2,1}}{w_{2,3}}|10\rangle\right)_{1,3}; \\ |v_2^{(1)}\rangle &= |0101\rangle - \frac{w_{2,2}}{w_{2,3}}|0110\rangle - \frac{w_{2,0}}{w_{2,1}}|1001\rangle + \frac{w_{2,0}w_{2,2}}{w_{2,1}w_{2,3}} \\ &= \left(|01\rangle - \frac{w_{2,0}}{w_{2,1}}|10\rangle\right)_{0,1} \left(|01\rangle - \frac{w_{2,2}}{w_{2,3}}|10\rangle\right)_{2,3}; \\ |v_3^{(1)}\rangle &= |0111\rangle - \frac{w_{3,0}}{w_{3,3}}|1110\rangle \\ &= \left(|01\rangle - \frac{w_{3,0}}{w_{3,3}}|10\rangle\right)_{0,3} |11\rangle_{1,2}; \\ |v_4^{(1)}\rangle &= |1011\rangle - \frac{w_{3,1}}{w_{3,3}}|1110\rangle \\ &= \left(|01\rangle - \frac{w_{3,1}}{w_{3,3}}|10\rangle\right)_{1,3} |11\rangle_{0,2}; \\ |v_5^{(1)}\rangle &= |1101\rangle - \frac{w_{3,2}}{w_{3,3}}|1110\rangle \\ &= \left(|01\rangle - \frac{w_{3,2}}{w_{3,3}}|10\rangle\right)_{2,3} |11\rangle_{0,1}. \end{aligned} \quad (74)$$

The eigenvectors can all be written in explicitly separable forms, where the indices outside the parentheses denotes the label partitions; note that these also match the second indices in the weight ratios. Evidently the the generalized zero eigenvectors for $n = 3$, Eqs. (63) and (68), can be written in a similar product form. This is due to the fact that the Hamiltonian (10) itself can be written as a sum of permutations of separable terms. For example, the terms in the $n = 4$ Hamiltonian that map $h = 2$ states to $h = 3$ states can be expressed as

$$\begin{aligned} \check{M}_{(h=2 \rightarrow 3)} &= \frac{1}{2} \left[()_{0,1} I_{2,3} + I_{0,1} ()_{2,3} + ()_{0,2} I_{1,3} + I_{0,2} ()_{1,3} \right. \\ &\quad \left. + ()_{0,3} I_{1,2} + I_{0,3} ()_{1,2} \right], \end{aligned} \quad (75)$$

where

$$\begin{aligned} ()_{i,j} &= |11\rangle_{i,j} (w_{2,i}\langle 01| + w_{2,j}\langle 10|)_{i,j}, \\ I_{i,j} &= (|01\rangle\langle 01| + |10\rangle\langle 10|)_{i,j}. \end{aligned} \quad (76)$$

The ‘identity’ operator is the sum of all idempotents with $h = 1$, enumerated by the $1/2$ prefactor in Eq. (75). Thus, $\check{M}_{(h=2 \rightarrow 3)}$ has the form of Cartesian products of operators over all four-site bipartitions restricted to states with specific Hamming weight. It is straightforward to verify that the $|v_1^{(1)}\rangle$ and $|v_2^{(1)}\rangle$ in Eq. (74) are zero eigenvectors of the first and second Cartesian product, respectively, and have no support on the third. Similar expressions can be obtained for the other terms in the Hamiltonian.

Construction of A_1 and B_1 proceeds analogously to the $n = 3$ case, and generates $\check{M}^{(2)} = B_1 A_1$ with basis states

(graph vertices) $\{|0011\rangle, |0101\rangle, |0111\rangle, |1011\rangle, |1101\rangle\}$ removed. However, all but one of the 23 non-zero terms in the resulting matrix is unique. From the graph perspective, only 5 edges are reweighted, 9 edges have unchanged weights, and 9 new edges with unique weights must be added. Generically, in the bosonic case, the number of unique terms that need to be evaluated during the row reduction procedure grows exponentially with n . There doesn't appear to be any way to exploit the separable nature of the generalized zero eigenvectors to simplify the calculation.

VI. DISCUSSION: PROSPECTS FOR A QUANTUM ALGORITHM

As discussed in Sec. IIIB, the permanent of an $n \times n$ matrix M relates to the eigenvalues of another 2^n -dimensional matrix \tilde{M} or \check{M} (the dimension of the latter is one smaller so that one basis state is unused). This matrix has several attributes that would appear to favor the development of an efficient quantum algorithm for the evaluation of the permanent: the dimension of \tilde{M} is a power of two, which would be the case for an n -qubit operator; matrix elements of \tilde{M} are easily indexed by address, which correspond to their original positions in M ; \tilde{M} is n -sparse (no row or column has more than $n-1$ elements); and the permanent is the maximal eigenvalue of \tilde{M}^n . Despite these nice features, however, the construction of an efficient algorithm for the permanent using this approach is not straightforward for one principal reason: neither \tilde{M} nor \check{M} is Hermitian or unitary.

As a first attempt at a quantum algorithm, one might leverage the relation $P_n = \langle 0 | \tilde{M}^n | 0 \rangle$, Eq. (31). The quantity on the right-hand side can be computed using any of the known algorithms for evaluating expectation values [35, 36]. Unfortunately, such algorithms have $O(1/\epsilon)$ or worse dependence on additive error [37], and thus an even worse dependence on the multiplicative error. Moreover, the operator norm of \tilde{M}^n is not polynomially bounded in general. Consequently, this approach fails to suggest an avenue toward an efficient quantum algorithm.

A more lucrative approach might be to make use of the fact that all non-zero eigenvalues of \tilde{M} have absolute value $|P_n|^{1/n}$, Eq. (23). Thus, if there exists an efficient procedure to generate one of the corresponding eigenstates, then $|P_n|^{1/n}$ can be computed efficiently to constant or polynomially small additive error. Note that an additive approximation of $|P_n|^{1/n}$ provides significantly more resolution, at least for the unitary matrices M that would be relevant to boson sampling, in contrast to an additive approximation of $|P_n|$. As noted by Aaronson

and Arkhipov [7], since $|P_n|$ is typically exponentially small for unitary matrices sampled from a Haar random distribution, an additive approximation of $|P_n|$ to polynomial accuracy would almost always return zero. On the other hand, the average of $|P_n|^{1/n}$ is in $\Omega(1)$ for unitary matrices sampled from a Haar random distribution, and therefore an approximation of $|P_n|^{1/n}$ to polynomially small or even constant additive error provides more resolution.

Unfortunately, generating any eigenstates of \check{M} , Eq. (21), is not straightforward. The coefficients in the linear combination depend on the value of P_n , which is unknown and in fact the goal of the computation. Even if one could obtain a sufficiently good approximation of P_n (via randomized classical algorithms), taking appropriate linear combinations using the techniques developed in Ref. [38] would only generate the targeted eigenstate with exponentially small probability, limiting the runtime of the algorithm. Specifically, it is not obvious how to adapt block-encoding techniques [39] to generate, with high probability, the state $\check{M}^{n-1}|0\rangle/\|\check{M}^{n-1}|0\rangle\|$, which is one of the terms in the desired linear combination.

Consider instead leveraging the useful property that the state $|0\rangle$ is an equal superposition of all eigenstates corresponding to non-zero eigenvalues of \tilde{M} . If \tilde{M} were unitary, this fact would have been sufficient for computing all eigenvalues of \tilde{M} efficiently using repeated application of the phase estimation algorithm [40]. Unfortunately, the extension of phase estimation to non-unitary operators is generally inefficient [41]. For the present problem, we expect phase estimation to take an exponentially long time, as the eigenvalues being estimated lie well inside the unit circle.

A more sophisticated approach to computing the eigenvalues of \tilde{M} is based on quantum linear-system solvers [42]. The complexity of this approach is limited by the condition number of the eigenvectors, however. We have verified numerically that the condition number is exponentially large for typical real and complex matrices M .

To summarize, mapping the problem of computing the permanent of M to calculating the eigenvalues of \tilde{M} would seem to suggest new routes for designing an efficient quantum algorithm to obtain a multiplicative approximation of the permanent. Yet, such an algorithm does not follow from the immediate application of the currently available algorithmic tools for linear algebra in a quantum setting. In all likelihood, if such an algorithm exists, it would rely on more subtle properties of the permanent than are made apparent by the present mapping.

Appendix A: Block-diagonal representation

This section derives the expression for \tilde{M}^{n+1} , where \tilde{M} is defined by Eq. (9). Consider first \tilde{M}^2 :

$$\begin{aligned}\tilde{M}^2 &= \left(\sum_{\mathbf{i}_0} \sum_{j_0=0}^{n-1} w_{h(\mathbf{i}_0),j_0} \sigma_{j_0}^+ |\mathbf{i}_0\rangle \langle \mathbf{i}_0| + |\mathbf{0}\rangle \langle \mathbf{1}| \right) \left(\sum_{\mathbf{i}_1} \sum_{j_1=0}^{n-1} w_{h(\mathbf{i}_1),j_1} \sigma_{j_1}^+ |\mathbf{i}_1\rangle \langle \mathbf{i}_1| + |\mathbf{0}\rangle \langle \mathbf{1}| \right) \\ &= \sum_{\mathbf{i}_0, \mathbf{i}_1} \sum_{j_0, j_1} w_{h(\mathbf{i}_0),j_0} \sigma_{j_0}^+ |\mathbf{i}_0\rangle \langle \mathbf{i}_0| w_{h(\mathbf{i}_1),j_1} \sigma_{j_1}^+ |\mathbf{i}_1\rangle \langle \mathbf{i}_1| + \sum_{\mathbf{i}_1} \sum_{j_1} |\mathbf{0}\rangle \langle \mathbf{1}| w_{h(\mathbf{i}_1),j_1} \sigma_{j_1}^+ |\mathbf{i}_1\rangle \langle \mathbf{i}_1| + \sum_{\mathbf{i}_0} \sum_{j_0} w_{h(\mathbf{i}_0),j_0} \sigma_{j_0}^+ |\mathbf{i}_0\rangle \langle \mathbf{i}_0| |\mathbf{0}\rangle \langle \mathbf{1}|.\end{aligned}\quad (\text{A1})$$

For the evaluation of the $\langle \mathbf{i}_0 | w_{h(\mathbf{i}_1),j_1} \sigma_{j_1}^+ | \mathbf{i}_1 \rangle$ factor in first term of Eq. (A1), there are three possibilities: $\sigma_{j_1}^+ | \mathbf{i}_1 \rangle = 0$, $\sigma_{j_1}^- | \mathbf{i}_0 \rangle = 0$, or $\sigma_{j_1}^+ | \mathbf{i}_1 \rangle = | \mathbf{i}_0 \rangle$ (equivalently $| \mathbf{i}_1 \rangle = \sigma_{j_1}^- | \mathbf{i}_0 \rangle$ or $\langle \mathbf{i}_1 | = \langle \mathbf{i}_0 | \sigma_{j_1}^+$), and the first two possibilities contribute nothing to the sum. Similar arguments apply to the second and third terms, and one obtains

$$\tilde{M}^2 = \sum_{\mathbf{i}} \sum_{j_0, j_1} w_{h(\mathbf{i}),j_0} w_{h(\mathbf{i}-1,j_1)} \sigma_{j_0}^+ | \mathbf{i} \rangle \langle \mathbf{i} | \sigma_{j_1}^+ + \sum_{j_0} (w_{n-1,j_0} | \mathbf{0} \rangle \langle \mathbf{1} | \sigma_{j_1}^+ + w_{0,j_0} \sigma_{j_0}^+ | \mathbf{0} \rangle \langle \mathbf{1} |). \quad (\text{A2})$$

Next consider \tilde{M}^3 . After elementary algebra along the same lines as above, one obtains

$$\begin{aligned}\tilde{M}^3 &= \sum_{\mathbf{i}} \sum_{j_0, j_1, j_2} (w_{h(\mathbf{i}),j_0} \sigma_{j_0}^+) | \mathbf{i} \rangle \langle \mathbf{i} | (w_{h(\mathbf{i}-1,j_1)} \sigma_{j_1}^+) (w_{h(\mathbf{i}-2,j_2)} \sigma_{j_2}^+) + \sum_{j_0, j_1} (w_{0,j_0} \sigma_{j_0}^+) (w_{1,j_1} \sigma_{j_1}^+) | \mathbf{0} \rangle \langle \mathbf{1} | \\ &+ \sum_{j_{n-1}, j_{n-2}} | \mathbf{0} \rangle \langle \mathbf{1} | (w_{n-1,j_{n-1}} \sigma_{j_{n-1}}^+) (w_{n-2,j_{n-2}} \sigma_{j_{n-2}}^+) + \sum_{j_0, j_{n-1}} (w_{0,j_0} \sigma_{j_0}^+) | \mathbf{0} \rangle \langle \mathbf{1} | (w_{n-1,j_{n-1}} \sigma_{j_{n-1}}^+).\end{aligned}\quad (\text{A3})$$

The form of leading term in \tilde{M}^{n+1} should now be evident:

$$\sum_{\mathbf{i}} \sum_{j_0, \dots, j_n} (w_{h(\mathbf{i}),j_0} \sigma_{j_0}^+) | \mathbf{i} \rangle \langle \mathbf{i} | (w_{h(\mathbf{i}-1,j_1)} \sigma_{j_1}^+) \cdots (w_{h(\mathbf{i}-n,j_n)} \sigma_{j_n}^+). \quad (\text{A4})$$

In the above expression, the $\langle \mathbf{i} | \prod_k \sigma_{j_k}^+$ term is zero unless $\mathbf{i} = \mathbf{1}$, but then $\sigma_{j_0}^+ | \mathbf{i} \rangle = 0$, so that the leading term vanishes. The remaining terms are straightforward generalizations of those found in Eqs. (A2) and (A3), and one obtains

$$\begin{aligned}\tilde{M}^{n+1} &= \sum_{j_0, \dots, j_{n-1}} \left[(w_{0,j_0} \sigma_{j_0}^+) \cdots (w_{n-1,j_{n-1}} \sigma_{j_{n-1}}^+) | \mathbf{0} \rangle \langle \mathbf{1} | + (w_{0,j_0} \sigma_{j_0}^+) \cdots (w_{n-2,j_{n-2}} \sigma_{j_{n-2}}^+) | \mathbf{0} \rangle \langle \mathbf{1} | (w_{n-1,j_{n-1}} \sigma_{j_{n-1}}^+) \right. \\ &+ \dots + (w_{0,j_0} \sigma_{j_0}^+) | \mathbf{0} \rangle \langle \mathbf{1} | (w_{1,j_1} \sigma_{j_1}^+) \cdots (w_{n-1,j_{n-1}} \sigma_{j_{n-1}}^+) + | \mathbf{0} \rangle \langle \mathbf{1} | (w_{0,j_0} \sigma_{j_0}^+) \cdots (w_{n-1,j_{n-1}} \sigma_{j_{n-1}}^+) \left. \right].\end{aligned}\quad (\text{A5})$$

A corollary is that the expression for arbitrary powers p is

$$\begin{aligned}\tilde{M}^p &= \sum_{\mathbf{i}} \sum_{j_0, \dots, j_{p-1}} (w_{h(\mathbf{i}),j_0} \sigma_{j_0}^+) | \mathbf{i} \rangle \langle \mathbf{i} | (w_{h(\mathbf{i}-1,j_1)} \sigma_{j_1}^+) \cdots (w_{h(\mathbf{i}-p+1,j_{p-1})} \sigma_{j_{p-1}}^+) \\ &+ \sum_{j_0, \dots, j_{p-2}} \left[(w_{0,j_0} \sigma_{j_0}^+) \cdots (w_{p-2,j_{p-2}} \sigma_{j_{p-2}}^+) | \mathbf{0} \rangle \langle \mathbf{1} | + (w_{0,j_0} \sigma_{j_0}^+) \cdots (w_{p-3,j_{p-3}} \sigma_{j_{p-3}}^+) | \mathbf{0} \rangle \langle \mathbf{1} | (w_{p-2,j_{p-2}} \sigma_{j_{p-2}}^+) \right. \\ &+ \dots + | \mathbf{0} \rangle \langle \mathbf{1} | (w_{n-1,j_0} \sigma_{j_0}^+) \cdots (w_{n-p+1,j_{p-2}} \sigma_{j_{p-2}}^+) \left. \right],\end{aligned}\quad (\text{A6})$$

which can be used to prove Eq. (14), i.e. that

$$\tilde{M}_m = \tilde{M}^m | \mathbf{0} \rangle \langle \mathbf{0} | \tilde{M}^{n-m+1}. \quad (\text{A7})$$

First,

$$\tilde{M}^p | \mathbf{0} \rangle = \sum_{\mathbf{i}} \sum_{j_0, \dots, j_{p-1}} (w_{h(\mathbf{i}),j_0} \sigma_{j_0}^+) | \mathbf{i} \rangle \langle \mathbf{i} | (w_{h(\mathbf{i}-1,j_1)} \sigma_{j_1}^+) \cdots (w_{h(\mathbf{i}-p+1,j_{p-1})} \sigma_{j_{p-1}}^+) | \mathbf{0} \rangle. \quad (\text{A8})$$

Only bitstrings \mathbf{i} with Hamming weight $p - 1$ will contribute, so

$$\tilde{M}^p|\mathbf{0}\rangle = \sum_{j_0, \dots, j_{p-1}} (w_{0,j_0} \sigma_{j_0}^+) (w_{1,j_1} \sigma_{j_1}^+) \cdots (w_{p-1,j_{p-1}} \sigma_{j_{p-1}}^+) |\mathbf{0}\rangle. \quad (\text{A9})$$

Second, following similar reasoning,

$$\begin{aligned} \langle \mathbf{0} | \tilde{M}^q &= \sum_{\mathbf{i}} \sum_{j_0, \dots, j_{q-1}} \langle \mathbf{0} | w_{h(\mathbf{i}), j_0} \sigma_{j_0}^+ | \mathbf{i} \rangle \langle \mathbf{i} | (w_{h(\mathbf{i})-1, j_1} \sigma_{j_1}^+) \cdots (w_{h(\mathbf{i})-q+1, j_{q-1}} \sigma_{j_{q-1}}^+) \\ &+ \sum_{j_0, \dots, j_{q-2}} \langle \mathbf{1} | (w_{n-1, j_0} \sigma_{j_0}^+) \cdots (w_{n-q+1, j_{q-2}} \sigma_{j_{q-2}}^+) \\ &= \sum_{j_0, \dots, j_{q-2}} \langle \mathbf{1} | (w_{n-1, j_0} \sigma_{j_0}^+) \cdots (w_{n-q+1, j_{q-2}} \sigma_{j_{q-2}}^+) \rangle. \end{aligned} \quad (\text{A10})$$

Putting these results together:

$$\begin{aligned} \tilde{M}^m |\mathbf{0}\rangle \langle \mathbf{0} | \tilde{M}^{n-m+1} &= \sum_{\substack{j_0, \dots, j_{m-1} \\ k_0, \dots, k_{n-m-1}}} (w_{0,j_0} \sigma_{j_0}^+) (w_{1,j_1} \sigma_{j_1}^+) \cdots (w_{m-1,j_{m-1}} \sigma_{j_{m-1}}^+) |\mathbf{0}\rangle \\ &\times \langle \mathbf{1} | (w_{n-1,k_0} \sigma_{k_0}^+) (w_{n-2,k_1} \sigma_{k_1}^+) \cdots (w_{m,k_{n-m-1}} \sigma_{k_{n-m-1}}^+) \\ &= \sum_{j_0, \dots, j_{n-1}} (w_{0,j_0} \sigma_{j_0}^+) (w_{1,j_1} \sigma_{j_1}^+) \cdots (w_{m-1,j_{m-1}} \sigma_{j_{m-1}}^+) |\mathbf{0}\rangle \\ &\times \langle \mathbf{1} | (w_{n-1,j_m} \sigma_{j_m}^+) (w_{n-2,j_{m+1}} \sigma_{j_{m+1}}^+) \cdots (w_{m,j_{n-1}} \sigma_{j_{n-1}}^+) \rangle. \end{aligned} \quad (\text{A11})$$

Comparison with the terms in Eq. (11) immediately yields

$$\tilde{M}_m = \tilde{M}^m |\mathbf{0}\rangle \langle \mathbf{0} | \tilde{M}^{n-m+1}. \quad (\text{A12})$$

-
- | | |
|---|--|
| <p>[1] A. Björklund, T. Husfeldt, and M. Koivisto, SIAM Journal on Computing 39, 546 (2009).</p> <p>[2] D. Cvetković, I. Gutman, and N. Trinajstić, Chemical Physics Letters 16, 614 (1972).</p> <p>[3] O. J. Heilmann and E. H. Lieb, Communications in Mathematical Physics 25, 190 (1972).</p> <p>[4] D. Schaub, Journal of Advances in Information Fusion 12, 20 (2017).</p> <p>[5] S. Scheel and S. Y. Buhmann, Acta Physica Slovaca 58, 675 (2008).</p> <p>[6] S. Aaronson, Proceedings of the Royal Society A 467, 3393 (2011).</p> <p>[7] S. Aaronson and A. Arkhipov, in <i>Proceedings of the Forty-Third Annual ACM Symposium on Theory of Computing</i> (Association for Computing Machinery, New York, NY, USA, 2011), STOC '11, pp. 333–342.</p> <p>[8] T.-C. Wei and S. Severini, Journal of Mathematical Physics 51, 092203 (2010).</p> <p>[9] V. Fisikopoulos and L. Peñaranda, Computational Geometry 54, 1 (2016).</p> <p>[10] L. G. Valiant, SIAM Journal on Computing 8, 410 (1979).</p> <p>[11] L. Valiant, Theoretical Computer Science 8, 189 (1979).</p> | <p>[12] A. Ben-Dor and S. Halevi, in <i>The 2nd Israel Symposium on Theory and Computing Systems</i> (1993), pp. 108–117.</p> <p>[13] S. Toda, SIAM Journal on Computing 20, 865 (1991).</p> <p>[14] D. G. Glynn, European Journal of Combinatorics 31, 1887 (2010).</p> <p>[15] X. Niu, S. Su, and J. Zheng, IOP Conference Series: Materials Science and Engineering 790, 012057 (2020).</p> <p>[16] M. Jerrum, A. Sinclair, and E. Vigoda, J. ACM 51, 671 (2004).</p> <p>[17] L. Eldar and S. Mehraban, in <i>2018 IEEE 59th Annual Symposium on Foundations of Computer Science (FOCS)</i> (2018), pp. 23–34.</p> <p>[18] A. Barvinok, Discrete & Computational Geometry 18, 205 (1997).</p> <p>[19] L. Gurvits and A. Samorodnitsky, Discrete & Computational Geometry 27, 531 (2002).</p> <p>[20] L. Gurvits, in <i>Mathematical Foundations of Computer Science 2005</i>, edited by J. Jędrzejowicz and A. Szepietowski (Springer Berlin Heidelberg, Berlin, Heidelberg, 2005), pp. 447–458.</p> <p>[21] F. Arute, K. Arya, R. Babbush, D. Bacon, J. C. Bardin, R. Barends, R. Biswas, S. Boixo, F. G. S. L. Brandao, D. A. Buell, et al., Nature 574, 505 (2019).</p> |
|---|--|

- [22] H.-S. Zhong, H. Wang, Y.-H. Deng, M.-C. Chen, L.-C. Peng, Y.-H. Luo, J. Qin, D. Wu, X. Ding, Y. Hu, et al., *Science* **370**, 1460 (2020).
- [23] L. S. Madsen, F. Laudenbach, M. F. Askarani, F. Rortais, T. Vincent, J. F. F. Bulmer, F. M. Miatto, L. Neuhaus, L. G. Helt, M. J. Collins, et al., *Nature* **606**, 75 (2022).
- [24] E. Knill, *Fermionic linear optics and matchgates* (2001), arXiv/quant-ph/0108033.
- [25] B. M. Terhal and D. P. DiVincenzo, *Phys. Rev. A* **65**, 032325 (2002).
- [26] L. Valiant, *SIAM J. Comput.* **31**, 1229 (2002).
- [27] D. P. DiVincenzo and B. M. Terhal, *Found. Phys.* **35**, 1967 (2005).
- [28] R. Jozsa and A. Miyake, *Proc. Royal Soc. A* **464**, 3089 (2008).
- [29] B. Grenet, *An upper bound for the permanent versus determinant problem* (2012), <https://www.lirmm.fr/~grenet/publis/Gre11.pdf>.
- [30] P. Bürgisser, *Séminaire Lotharingien de Combinatoire* **75**, B75a (2016).
- [31] J. M. Landsberg and N. Ressayre, in *Proceedings of the 2016 ACM Conference on Innovations in Theoretical Computer Science* (Association for Computing Machinery, New York, NY, USA, 2016), pp. 29–35.
- [32] J. Hüttelhain and C. Ikenmeyer, *Linear Algebra and its Applications* **504**, 559 (2016).
- [33] D. S. Watkins, *SIAM Review* **47**, 3 (2005).
- [34] T. Zaslavsky, *Discrete Applied Mathematics* **4**, 47 (1982).
- [35] E. Knill, G. Ortiz, and R. D. Somma, *Phys. Rev. A* **75**, 012328 (2007).
- [36] P. Rall, *Phys. Rev. A* **102**, 022408 (2020).
- [37] A. Alase, R. R. Nerem, M. Bagherimehrab, P. Høyer, and B. C. Sanders, *Phys. Rev. Research* **4**, 023237 (2022).
- [38] D. W. Berry, A. M. Childs, and R. Kothari, in *2015 IEEE 56th annual symposium on foundations of computer science* (IEEE, 2015), pp. 792–809.
- [39] G. H. Low and I. L. Chuang, *Quantum* **3**, 163 (2019), ISSN 2521-327X.
- [40] D. S. Abrams and S. Lloyd, *Phys. Rev. Lett.* **83**, 5162 (1999).
- [41] H. Wang, L.-A. Wu, Y.-x. Liu, and F. Nori, *Phys. Rev. A* **82**, 062303 (2010).
- [42] C. Shao, *ACM Transactions on Quantum Computing* **3** (2022).